Received: 9 October 2019 | Accepted: 29 November 2019

DOI: 10.1002/asjc.2312

REGULAR PAPER

WILEY

Comparative analysis of model reduction strategies for circuit based periodic control problems

Mohammad-Sahadet Hossain[1] | **Aniqa Tahsin**[2] | **Sufi Galib Omar**[2] | **Ekram Hossain Khan**[2]

[1]Department of Mathematics and Physics, North South University, Dhaka, Bangladesh

[2]Department of Electrical and Computer Engineering, North South University, Dhaka, Bangladesh

Correspondence
Aniqa Tahsin, Department of Electrical and Computer Engineering, North South University, Dhaka, Bangladesh.
Email: atahsin1828@gmail.com

Abstract

This paper is a comparative analysis of two prominent iterative algorithms for model order reduction of linear time-varying (LTV) periodic systems where the system's matrices are singular. Our proposed method is based on a reformulation of the LTV model to an equivalent linear time-invariant (LTI) model using a suitable discretization procedure. The resulting LTI model is reduced in two ways, once by applying a balanced truncation method and once by applying a Krylov-based method known as iterative rational Krylov algorithm (IRKA). During the application of balanced truncation, the low-rank Cholesky factorized alternating directions implicit (LRCF-ADI) method is used to estimate the solutions of the corresponding LTI form of Lyapunov equations. Since the system's matrices are singular, the concept of pseudo-inverse is adopted to compute the shift parameters needed in the LRCF-ADI iterations. For the Krylov-based IRKA, our work is twofold. We solve the time-invariant Lyapunov equation for the observability Gramian and apply a moment-matching Krylov technique. The accuracy and effectiveness of the two proposed techniques are demonstrated with the help of frequency response graphs, bode plots, and eigenstructure of the main and reduced models.

KEYWORDS

balanced truncation, IRKA, LRCF-ADI, LTV system, model order reduction (MOR)

1 | INTRODUCTION

Dynamical systems are extensively used in the modeling of physical processes and systems such as temperature control, circuit simulations, structural dynamics, industrial applications, and microelectro-mechanical systems (MEMS) [1–3]. The ever-increasing dimensions and complexity of the models used to represent these dynamical systems stems the need to precisely and efficiently simulate the behavior of the dynamical systems. Numerically simulating and optimizing these complicated models requires high numerical effort, time-consuming computations, and sufficient memory space. To alleviate these computation burdens, we can use model order reduction (MOR) to approximate a simpler yet precise version of the original model. The smaller model mimics the input-output behavior of the original system. In addition, the smaller model preserves significant characteristics of the original model.

Let us consider the continuous periodic linear time-varying descriptor system where the system's dynamics change with time t. Such a system can be represented

in the more general state-space form as,

$$\begin{aligned} E(t)\dot{x}(t) &= A(t)x(t) + B(t)u(t), \\ y(t) &= C(t)x(t) + D(t)u(t), \end{aligned} \tag{1}$$

where $x(t) \in \mathbb{R}^{\mathfrak{n}}$, $u(t)$ and $y(t)$ represent the descriptor vector, input of the system, and output of the system, respectively, and $\mathfrak{n}$ is the order of the system. All the matrices in this system change with time and they are periodic with a time period T. At any point of time, $E(t)$ and $A(t)$ can be singular. We, in general, write system (1) omitting the matrix $D(t)$ as it does not have any effect on the dynamics of the system.

Analysis of LTV systems can be cumbersome and tricky, especially when large-scale systems are involved. To ease the computational complexity, we can convert the linear time-varying system (1) into its equivalent LTI form. This reformulation also allows us to extend theory dedicated to time-invariant systems to the LTV setting [4–6]. It is important to note that this type of LTI conversion is possible for a system which has near linear response but is nonlinear in nature (sometimse called weakly nonlinear). That means systems have small periodic perturbation [5–7].

Using a suitable discretization scheme, such as the Euler discretization discussed in [4], we can find the LTI version of the corresponding time-varying system (1). A multi-input and multi-output (MIMO) LTI system has the general form,

$$\begin{aligned} E\dot{x}(t) &= Ax(t) + Bu(t), \\ y(t) &= Cx(t), \end{aligned} \tag{2}$$

where $x(t) \in \mathbb{R}^{\mathfrak{n}}$, $u(t) \in \mathbb{R}^{\mathfrak{p}}(\mathfrak{p} \leq \mathfrak{n})$, $y(t) \in \mathbb{R}^{\mathfrak{q}}$. There are $\mathfrak{p}$ inputs and $\mathfrak{q}$ outputs in the system. The system's matrices $E, A \in \mathbb{R}^{\mathfrak{n}\times\mathfrak{n}}$, $B \in \mathbb{R}^{\mathfrak{n}\times\mathfrak{p}}$ and $C \in \mathbb{R}^{\mathfrak{q}\times\mathfrak{n}}$ do not change with time. If there is a single input and a single output, the system can be identified as a SISO system where $\mathfrak{p} = 1$ and $\mathfrak{q} = 1$. B and C will then be modified to b and c^T, respectively.

Once the LTI system is found, we approximate the reduced order model of this corresponding system,

$$\begin{aligned} \check{E}\dot{\check{x}}(t) &= \check{A}\check{x}(t) + \check{B}u(t), \\ \check{y}(t) &= \check{C}\check{x}(t), \end{aligned} \tag{3}$$

where $\check{E}, \check{A} \in \mathbb{R}^{\mathfrak{r}\times\mathfrak{r}}$, $\check{B} \in \mathbb{R}^{\mathfrak{r}\times\mathfrak{p}}$, $\check{C} \in \mathbb{R}^{\mathfrak{q}\times\mathfrak{r}}$ are the system matrices of the reduced model with an order $\mathfrak{r}(\mathfrak{r} << \mathfrak{n})$. The reduced model is then used for simulations, decision making, predictions, and quick analysis of the original model in very efficient time. In addition to having smaller dimensions, the reduced model retains important characteristics of the main model such as stability and passivity.

Model reduction of (1) has been the topic of intensive research in recent years. Attempts have been made to reduce the dimensions of large-scale systems using balanced truncation [8–12], Krylov-based projection methods [1,5,13–16], the interpolatory method, optimal Hankel norm method, and polynomial method, as seen in [17]. Model reduction algorithms linking both balanced truncation and Krylov-based methods have also been proposed in [2,18–21]. For example, [18] demonstrates how a balanced truncation technique based on Krylov subspace methods can be applied to a general large-scale RLC network. The Krylov subspace method was used to approximate the lowrank square roots of the original system's Gramians. Similarly, in [19], a combination of the Rational Krylov Subspace Method (RKSM) and Alternating Direction Implicit (ADI) methods were employed to approximate the solutions of Lyapunov equations. Although there is existing research work that combines aspects of balanced truncation and Krylov-based methods, a direct comparison between the two methods [22–25] is rather limited. For example, in [23], a qualitative comparison between Krylov subspace methods, balanced truncation, and mode displacement methods was performed. The results revealed that only the balanced truncation method produced a better approximation of the original model than the other two methods at high frequencies. Likewise, in [24], a Krylov-subspace approach and balanced truncation were both applied to a power system and results showed that the Krylov-subspace method generated a model that was less accurate at high frequencies. Due to the computational complexities that arise in the application of these suggested reduction methods, we have proposed two iterative techniques that implement balanced truncation and Krylov subspace methods in a more efficient manner.

The remainder of this paper is organized as follows. In Section 2, we show a backward Euler based discretization scheme to reformulate our continuous time-varying system to a time-invariant system. In Section 3, we introduce and compare two important approaches for model reduction: balanced truncation and Krylov subspace methods. After a detailed outline of the proposed algorithms in Section 4, the numerical results obtained from MATLAB simulations are presented in Section 5. Finally, we conclude and discuss future work in Section 6.

2 | PROBLEM FORMULATION

The reduction strategy is based on finding an equivalent LTI representation of the LTV model using some suitable discretization schemes. In this section, we present a discussion of the reduced order modeling framework of the LTV systems.

2.1 | LTI systems

The Laplace transformation of the LTI system (2) results in its frequency domain version, which transforms to the following transfer function,

$$H(s) = C(sE - A)^{-1}B. \tag{4}$$

In this paper we consider only the stable systems, that means for the LTI system (2), the eigenvalues of its pencil $(\lambda E - A)$ must be taken into consideration. The system is considered to be stable if all the eigenvalues lie in the left half of the plane. The system is considered to be regular if its determinant, that is, det $(\lambda E - A)$ is nonzero.

2.2 | Analysis of circuit based LTV systems

Let us consider a nonlinear circuit system where two signals are present: b_l and $u(t)$. In terms of magnitude, b_l is larger than $u(t)$. An output $\mathsf{z}(t)$ is generated from the two signals. For convenience, $u(t)$ and $\mathsf{z}(t)$ are scalars. The following differential-algebraic equation (DAE) can used to describe the nonlinear circuit equations [4].

$$\begin{aligned} f(v(t)) + \frac{dq_c(v(t))}{dt} &= Bu(t) + b_l(t), \\ \mathsf{z}(t) &= c^T v(t). \end{aligned} \tag{5}$$

In the above equation, $u(t)$ is the input source and $v(t)$ describes the branch currents and nodal voltages. Here $f()$ and $q_c()$ represent the nonlinear resistive and flux/charge terms, respectively. The input and output are connected to the remaining part of the system by vectors found in $B(t)$ and $C(t)$.

In (5), the total quantities are represented by the variables $v(t)$ and $u(t)$. Separating $v(t)$ and $u(t)$ into two portions, a small and a large signal portion,

$$u = u^{(\mathscr{L})} + u^{(\mathfrak{s})}, \qquad v = v^{(\mathscr{L})} + v^{(\mathfrak{s})},$$

and then linearizing around the large signal portion $v^{(\mathscr{L})}$, we get the following LTV model [4].

$$\mathscr{G}(t)v^{(\mathfrak{s})} + \frac{d}{dt}(\mathfrak{C}(t)v^{(\mathfrak{s})}) = Bu^{(\mathfrak{s})}(t), \tag{6}$$

where for the small response $v^{(\mathfrak{s})}$, $\mathfrak{C}(t) = \partial q_c(v^{(\mathscr{L})})(t)/\partial v^{(\mathfrak{s})}$ is the capacitance matrix and $\mathscr{G}(t) = \partial f(v^{(\mathscr{L})})(t)/\partial v^{(\mathscr{L})}$ is the conductance matrix. We can omit the superscript and write (6) as

$$\mathscr{G}(t)v + \frac{d}{dt}(\mathfrak{C}(t)v) = Bu(t). \tag{7}$$

Assuming $E(t) = \mathfrak{C}(t)$, $A(t) = -(\mathscr{G}(t) + \dot{\mathfrak{C}}(t))$, Equation (7) can be related to the standard notation.

2.3 | Discretization of transfer function

In the LTI case, model reduction is generally performed based on the rational estimations of the frequency-domain transfer function, as observed in many of the existing works. Following the formalism in [26], $v(t)$ can be written with the help of a time-varying transfer function,

$$v(t) = \int_{\infty}^{-\infty} h(i\dot{\omega}, t)\, u(\dot{\omega})\, e^{i\dot{\omega}t}\, \mathrm{d}\dot{\omega}, \tag{8}$$

where $h(i\dot{\omega}, t)$ is time-varying and $u(\dot{\omega})$ is the Fourier transform of $u(t)$. Using (8) and the notation $s = i\omega$, (7) can be used to compute $h(s, t)$ as,

$$\mathscr{G}(t)h(s,t) + \frac{d}{dt}(\mathfrak{C}(t)h(s,t)) + s\,\mathfrak{C}(t)h(s,t) = B. \tag{9}$$

Then the transfer function $\Phi(s, t)$ of system (1) (omitting $D(t)$) can be defined as,

$$\Phi(s,t) = C(t)\, h(s,t). \tag{10}$$

Assuming that $\Phi(s, t)$ is a rational function, we can obtain $\Phi(s, t)$ by discretizing (9). As the nature of our work deals with LTV systems, it is crucial to specify $B(t)$ and $C(t)$ over the fundamental period T. If we collocate $h(s, t)$ over time samples $t \in [0, T]$ at L sample time points $t_1, \ldots, t_L$, with periodicity $t_L = T$, we can find the time-domain form of (9). Implementing the backward Euler method discussed in [4], and taking into account the periodicity of $h(s, t)$, that is, $h(s, t) = h(s, t_L)$, (9) can be represented as,

$$(s\mathcal{E} - \mathcal{A})\,\mathcal{H}(s) = \mathcal{B}, \tag{11}$$

where,

$$\mathcal{A} = -(\mathcal{G} + \Delta\mathcal{E}),$$

$$\mathcal{G} = \begin{bmatrix} \mathscr{G}_1 & & & \\ & \mathscr{G}_2 & & \\ & & \ddots & \\ & & & \mathscr{G}_L \end{bmatrix},\ \mathcal{E} = \begin{bmatrix} \mathfrak{C}_1 & & & \\ & \mathfrak{C}_2 & & \\ & & \ddots & \\ & & & \mathfrak{C}_L \end{bmatrix};$$

$$\Delta = \begin{bmatrix} \frac{1}{\Delta_1}I & & & -\frac{1}{\Delta_1}I \\ -\frac{1}{\Delta_2}I & \frac{1}{\Delta_2}I & & \\ & \ddots & \ddots & \\ & & -\frac{1}{\Delta_L}I & \frac{1}{\Delta_L}I \end{bmatrix},$$

$$\mathcal{H}(s) = [h_1^T(s), h_2^T(s), \ldots, h_L^T(s)]^T,$$

$$\mathcal{B} = [B_1^T, B_2^T, \ldots, B_L^T]^T,$$

where, $\tilde{\mathscr{G}}_i = \tilde{\mathscr{G}}(t_i)$, $\tilde{\mathfrak{C}}_i = \tilde{\mathfrak{C}}(t_i)$, $B_i = B(t_i)$, $h_j(s) = h(s, t_i)$, and Δ_i is the i^{th} time step. Furthermore,

$$\mathcal{C} = [C_1\ C_2\ \ldots\ \ldots\ C_L]^T,$$

where $C_i = C(t_i)$. The baseband transfer functions $\mathcal{H}(s)$ is shown as [6],

$$\mathcal{H}(s) = \mathcal{C}(s\,\mathcal{E} - \mathcal{A})^{-1}\,\mathcal{B}. \tag{12}$$

The equation above is the time-domain version of an LTV transfer function. With the help of the discretization technique, the $\mathfrak{n}$ dimensional LTV system (1) has been transformed to its corresponding LTI system of dimension $N = \mathfrak{n}L$. It is important to note that the size of the original LTV system is smaller than the LTI system by a factor of L where L quantifies the time steps used in the discretization. For the model reduction of LTI systems, (12) can be directly used. Furthermore, any iterative methods for LTI systems can be applied to the matrices shown in (11)–(12).

3 | MODEL REDUCTION STRATEGIES

Throughout the years, a myriad of model order reduction strategies has emerged for the reduction of large-scale systems. These methods fall under two main categories: projection-based and non-projection based. Two commonly used projection-based reduction methods for very large-order systems are balanced truncation and Krylov subspace methods. In this section, we show the framework of both procedures together with the theoretical and numerical aspects.

3.1 | Balanced truncation MOR

One prominent projection-based reduction method is balanced truncation. In this method, the following set of matrix equations, formally known as Lyapunov equations, are required to be solved for a system similar to (2) with $E = I$, that is, an identity matrix.

$$\begin{aligned} A\mathcal{P} + \mathcal{P}A^T &= -BB^T, \\ A^T\mathcal{Q} + \mathcal{Q}A &= -C^TC. \end{aligned} \tag{13}$$

Here, $\mathcal{P}$ and $\mathcal{Q}$ are the solutions to (13). These solutions are unique positive definite. $\mathcal{P}$ and $\mathcal{Q}$ are known as the controllability and observability Gramians, respectively [27]. The controllability Gramian specifics the amount of input energy required to reach a specific state [27]. On the other hand, the observability Gramian quantifies the output energy. The main gist of balanced truncation is to balance the system in such a way that the states that are difficult to control are also difficult to observe and vice-versa. Once the system is balanced, the controllability and observability Gramians become diagonal and equal [27]. The states that do not play a major role in the system's dynamics are then eliminated. As a result, the dimensions of the system are reduced.

The Lyapunov equations and the related matrix equations play an indispensable role in numerous areas of control theory such as stability analysis, optimal control, and model order reduction [28,29]. These equations are also an integral part in power systems control and signal processing. Since Lyapunov equations are encountered in such an extensive range of applications, the solution of these equations are of great interest. Decades of research have brought forth various methods for solving the Lyapunov equations in its general form. These methods include the Bartels-Stewart method, alternating direction implicit (ADI) method, Hessenberg-Schur method, and Hammarling method [28].

3.1.1 | LRCF-ADI

The method of interest in this paper is the LRCF-ADI method, which is geared towards solving large-scale Lyapunov equations that have right-hand sides of low rank [30].

The generalized form of a Lyapunov equation is shown in (14),

$$\mathcal{A}X\mathcal{E}^T + \mathcal{E}X\mathcal{A}^T = -\mathcal{G}\mathcal{G}^T. \tag{14}$$

In order for the LRCF-ADI method to converge, the pencil of the system $(\lambda\mathcal{E} - \mathcal{A})$ must be c-stable, which signifies that all the finite eigenvalues of the pencil must possess negative real part. The performance and convergence rate of this method heavily relies on the shift parameters $p_1, p_2, p_3, \ldots, p_j$. Optimal ADI shift parameters can be determined by solving the following rational min-max problem [31],

$$\{p_1, p_2, .., p_j\} = \underset{p_1,p_2,\ldots,p_j \in \mathbb{C}^-}{\arg\min} \max_{t \in \mathrm{Sp}(\mathcal{E},\mathcal{A})} \prod_{i=1}^{j} \frac{|t - \bar{p}_j|}{|t + p_j|}, \tag{15}$$

where $(\mathcal{E}, \mathcal{A})$ denotes the spectrum of $\mathcal{E}^{-1}\mathcal{A}$. Computing optimal ADI shift parameters tends to be problematic because it involves expensive computations and spectral data that sometimes cannot be easily found. This is especially true when dealing with large-scale problems. Therefore, we use suboptimal ADI shift parameters that can be found using the heuristic approach explained in [32]. The heuristic approach makes use of the largest and smallest eigenvalues of the pencil $(\lambda\mathcal{E} - \mathcal{A})$ and these eigenvalues can be located using an Arnoldi iteration. The Arnoldi iteration is discussed in detail in the next section.

The generalized ADI iteration for (14) is given by

$$\begin{aligned} (\mathcal{A} + p_j\mathcal{E})X_{j-\frac{1}{2}} &= -\mathcal{G}\mathcal{G}^T - X_{j-1}(\mathcal{A}^T - p_j\mathcal{E}), \\ (\mathcal{A} + p_j\mathcal{E})X_j &= -\mathcal{G}\mathcal{G}^T - X^T_{j-\frac{1}{2}}(\mathcal{A}^T - p_j\mathcal{E}). \end{aligned} \tag{16}$$

We can note that the matrix $X_{j-\frac{1}{2}}$ is not symmetric after the initial step of each iteration. However, this matrix becomes symmetric once the second step is completed. The two steps in (16) can be combined into a single-step iteration

$$X_j = -2p_j(\mathcal{A}+p_j\mathcal{E})^{-1}\mathcal{G}\mathcal{G}^T(\mathcal{A}+p_j\mathcal{E})^{-T} + (\mathcal{A}+p_j\mathcal{E})^{-1} (\mathcal{A}-p_j\mathcal{E})X_{j-1}(\mathcal{A}-p_j\mathcal{E})^T(\mathcal{A}+p_j\mathcal{E})^{-T}. \tag{17}$$

Using the Cholesky Factorization $X_j = Z_j Z_j^T$, (17) can be rewritten in terms of Z_j as,

$$z_j = [\sqrt{-2p_1}(\mathcal{A}+p_j\mathcal{E})^{-1}\mathcal{G}, (\mathcal{A}+p_j\mathcal{E})^{-1}(\mathcal{A}-p_j\mathcal{E})Z_{j-1}],$$

For $j = 1$, $z_1 = \sqrt{-2p_1}((\mathcal{A}+p_j\mathcal{E})^{-1}\mathcal{G})$.

Therefore, it can be stated that (17) creates the Cholesky factors by adding a new column at each step. Assuming $X_0 = 0$ the Cholesky factor Z_j can be expressed as

$$Z_J = [z_J, P_{J-1}z_J, P_{J-2}(P_{J-1}z_J), \ldots \ldots, P_1(P_2 \ldots P_{J-1}z_J)], \tag{18}$$

where $P_i = \frac{\sqrt{-2\mathrm{Re}(p_i)}}{\sqrt{-2\mathrm{Re}(p_{i+1})}}(\mathcal{A}+p_i\mathcal{E})^{-1}(\mathcal{A}-p_{i-1}\mathcal{E})$.

Here, P_i is the step operator applied to compute the new column in each iteration. The iteration is repeated until a specified residual tolerance level is met. We can check the residual norm using the relation,

$$||\mathcal{A}X_j\mathcal{E}^T + \mathcal{E}X_j\mathcal{A}^T + \mathcal{G}\mathcal{G}^T|| < \epsilon, \tag{19}$$

where the residual tolerance is denoted by ϵ. Now, let us consider the following set of Lyapunov equations associated with the system (11),

$$\mathcal{A}P\mathcal{E}^T + \mathcal{E}P\mathcal{A}^T = -\mathcal{B}\mathcal{B}^T, \tag{20}$$

$$\mathcal{A}^T Q\mathcal{E} + \mathcal{E}^T Q\mathcal{A} = -\mathcal{C}^T\mathcal{C}. \tag{21}$$

As mentioned earlier, P and Q are solutions to the dual Lyapunov equations. If we approximate P and Q using the low rank Cholesky factors obtained from the LRCF-ADI method, we can decrease the computational complexity and required memory space [33].

The Cholesky factorizations of P and Q are computed as

$$P \approx \check{Z}_C\check{Z}_C^T, \quad Q \approx \check{Z}_O\check{Z}_O^T, \tag{22}$$

where $\check{Z}_C \in \mathbb{R}^{n\times m}$ and $\check{Z}_O \in \mathbb{R}^{n\times l}$ are the low rank Cholesky factors.

3.1.2 | Block Arnoldi iteration

As mentioned earlier, the largest and smallest eigenvalues of the pencil $(\lambda\mathcal{E}-\mathcal{A})$ are needed to determine the suboptimal ADI shift parameters of (18). To find these eigenvalues, the Arnoldi iteration is a suitable choice.

The Arnoldi iteration is often used to systematically construct an orthonormal base for a Krylov subspace. This orthonormal base can be represented by a matrix $\mathcal{W} = (w_1, \ldots, w_k) \in \mathbb{C}^{n\times k}$ where $\mathcal{W}^*\mathcal{W} = I$. Here $\mathcal{W}^*$ is denoted as the conjugate transpose of $\mathcal{W}$. $\mathcal{W} = \mathrm{span}\,(w_1, \ldots, w_k) = K_k(\mathcal{F}, b) = \mathrm{span}\,(\mathcal{F}, \mathcal{F}b, \ldots, \mathcal{F}^{k-1}b)$[34].

Here, $\mathcal{F} = \mathcal{E}^{-1}\mathcal{A}$ and b is an arbitrary vector that is necessary to get the Arnoldi iteration started. Due to the singularity of $\mathcal{E}$, the inverse of this matrix cannot be directly obtained. To overcome this issue, we used an additional method called pseudo-inverse [35].

Let us consider a Hessenberg matrix denoted by $\mathcal{H}$ where, $\mathcal{H} = \mathcal{W}^*\mathcal{F}\mathcal{W}$ and $\mathcal{H} \in \mathbb{C}^{k\times k}$. The eigenvalues of this Hessenberg matrix are identified as Ritz values. Since $\mathcal{H}$ is the orthogonal projection of $(\lambda\mathcal{E}-\mathcal{A})$, some of the Ritz values converge to the eigenvalues of the pencil. It has been observed that the Ritz values often converge to the eigenvalues positioned at the edge of the spectrum of the pencil [36].

Further details regarding the Arnoldi iteration can be found in [36]. Consider the following equations

$$\mathcal{F}\mathcal{W} = \mathcal{W}\mathcal{H} + \mathfrak{f}e_k, \tag{23}$$

$$\mathcal{H} = \mathcal{W}^T\mathcal{F}\mathcal{W}, \qquad \mathcal{W}^T\mathcal{W} = I_k, \qquad \mathcal{W}^T\mathfrak{f} = 0. \tag{24}$$

Here, $\mathcal{W}$ is the orthonormal vector matrix and $\mathcal{H}$ is the Hessenberg matrix as previously mentioned. $\mathfrak{f}$ represents the residual calculated at each step and e_k is the final column of I_k. Equations 23 and (24) are executed k number of iterations.

With the help of the Arnoldi iteration, we can find the large generalized eigenvalues of the pencil. To locate the small eigenvalues of the pencil, we can use an inverse Arnoldi iteration. In an inverse Arnoldi iteration, $\mathcal{F}$ is simply substituted with $\mathcal{F}^{-1}$. Executing the Arnoldi iteration and its inverse counterpart gives us two upper Hessenberg matrices that can be used to approximate the largest and smallest eigenvalues of the system.

3.1.3 | Formation of reduced model

Now that we have established a general idea of how we can solve the dual set of Lyapunov equations using the LRCF-ADI method, we can move on to the final steps of the balanced truncation procedure. Implementation of the LRCF-ADI method results in the low-rank version of the controllability and observability Gramians. Using these Gramians, we can find the Hankel singular values of the system as shown in the following equation,

$$\sigma_i(\Sigma) = \sqrt{\lambda_i(PQ)}. \tag{25}$$

Here, the Hankel singular values are denoted as σ_i. The importance of Hankel singular values lies in their ability to measure the amount of energy present in each state of the system. The Hankel singular values that are small in magnitude correspond to the states that are hard to control (reach) and hard to observe in the same time. These states have little impact on the system's input-output behavior and therefore can be eliminated. As a result, removal of

these trivial states from the original system leads to a reduced model [37].

Using the matrix $\mathcal{E}$ and the low-rank Cholesky factors of P and Q, the singular value decomposition can be computed as

$$U\Sigma V^T = \text{SVD}\,(\check{Z}_O^T \mathcal{E} \check{Z}_C). \tag{26}$$

Here, $U \in \mathbb{R}^{l\times l}$ and $V \in \mathbb{R}^{m\times m}$ are unitary matrices and $\Sigma \in \mathbb{R}^{l\times m}$ is a diagonal matrix. The most important feature of Σ is that its diagonal entries represent Hankel singular values that are organized in descending order.

By setting a tolerance level, the number of truncated Hankel singular values can be controlled. If r number of Hankel singular values can be retained without surpassing the tolerance level, then we can denote the first r columns of U and V as U_e and V_e where $U_e \in \mathbb{R}^{l\times r}$ and $V_e \in \mathbb{R}^{m\times r}$. Keeping only r number of Hankel singular values and removing the rest results in a reduced version of the diagonal matrix Σ. This reduced matrix can be written as Σ_e, where $\Sigma_e = \text{diag}\quad(\sigma_1, \sigma_2, \ldots \ldots \ldots \sigma_r) \in \mathbb{R}^{r\times r}$.

The truncation matrices shown in (27)

$$T_L = \check{Z}_O U_e \Sigma_e^{-1/2} \quad and \quad T_R = \check{Z}_C V_e \Sigma_e^{-1/2}, \tag{27}$$

can be applied to the system's matrices to obtain the reduced system where

$$\begin{aligned} \check{E} &= T_L^T \mathcal{E} T_R, & \check{A} &= T_L^T \mathcal{A} T_R, \\ \check{B} &= T_L^T \mathcal{B}, & \check{C} &= C T_R. \end{aligned} \tag{28}$$

For the reduced model (28) we can also generate a reduced transfer function $\check{H}(s)$ similar to (12). Stability is preserved in the reduced order. The H_∞ norm error bound in (29) can be used to check whether the transfer function of the reduced model is a good approximation of the original system's transfer function.

$$||\mathcal{H}(s) - \check{\mathcal{H}}(s)||_\infty \leq 2 \sum_{i=r+1}^{n} \sigma_i. \tag{29}$$

3.2 | Krylov based MOR

In recent years, Krylov subspace methods have emerged as one of the most useful tools for the model order reduction of linear systems. A fair amount of attention has been devoted to these methods due to their easy implementation and low computational cost. In Krylov subspace methods, the goal is to match a certain number of coefficients of the Taylor series expansion of the transfer functions of the original and reduced model around a specific frequency. These coefficients are known as *moments* [27]. If the series is expanded around a point where $s_o = \infty$, the coefficients are defined as Markov parameters [27]. Model order reduction using Krylov subspaces are also referred to as moment-matching techniques. Now we expand the transfer function (4) in terms of the Taylor series as,

$$\begin{aligned} H(s) = -CA^{-1}B - C(A^{-1}E)A^{-1}Bs - \ldots \\ \ldots - C(A^{-1}E)^i A^{-1}Bs^i. \end{aligned} \tag{30}$$

Krylov subspaces are the cornerstone of moment-matching techniques because these subspaces are required to generate projection matrices that are shown to form bases of the Krylov subspaces itself during moment-matching. Projection matrices are essential because a majority of MOR methods are implemented by means of projection. Let us consider the following projection,

$$x(t) = V\check{x}(t) + \epsilon(t), \tag{31}$$

where $V \in \mathbb{R}^{\mathfrak{n}\times r_{kry}}$ is the transformation matrix, $x(t) \in \mathbb{R}^{\mathfrak{n}}$ is the original state vector, $\check{x}(t) \in \mathbb{R}^{r_{kry}}$ is the reduced state vector, $\epsilon(t)$ is the residual, and $r_{kry} << \mathfrak{n}$. Substituting this projection to the system in Equation (2) and multiplying the state equations by a second transformation matrix $W \in \mathbb{R}^{\mathfrak{n}\times r_{kry}}$, where, $W^T\epsilon(t) = 0$, the following system with reduced order r_{kry} can be obtained.

$$\begin{aligned} W^T E V\dot{\check{x}}(t) = W^T A V\check{x}(t) + W^T B u(t), \\ y(t) = CV\check{x}(t). \end{aligned} \tag{32}$$

Therefore, the reduced system matrices are:

$$\begin{aligned} E_{r_{kry}} &= W^T EV, & A_{r_{kry}} &= W^T AV, \\ B_{r_{kry}} &= W^T B, & C_{r_{kry}} &= CV. \end{aligned} \tag{33}$$

Now that we have seen the role projection matrices play in model order reduction procedures, let us briefly describe how they are generated. As mentioned earlier, projection matrices form bases of Krylov subspaces during moment-matching. A standard Krylov subspace is spanned by the following succession of μ vectors as,

$$K_\mu(A, b) = span(b, Ab, A^2b, \ldots, A^{\mu-1}b), \tag{34}$$

where $A \in \mathbb{R}^{\mathfrak{n}\times\mathfrak{n}}$ and $b \in \mathbb{R}^{\mathfrak{n}}$ is identified as the initial vector [13]. The vectors $b, Ab, A^2b, \ldots, A^{\mu-1}b$, which build the subspace, are called basic vectors.

When b has more than one initial vector, (34) is formally known as block Krylov subspace. A basis of a Krylov subspace is created from the first linearly independent basic vectors [31].

There are two major algorithms that can be utilized to systematically construct the projection matrices V and W: the Arnoldi algorithm and the Lanczos algorithm. In a state-space system, there are two Krylov subspaces: an input Krylov subspace and an output Krylov subspace. One or both of the subspaces can be used in projection.

According to [16], if the columns of the projection matrices V and W both produce bases for the input and output Krylov subspaces, then the first 2μ moments of the original and reduced system are equivalent. Once the projection matrices are obtained, they can be applied to the system matrices of the original model, yielding a smaller model that contains a certain number of moments that are equivalent to the original system's moments.

Since Krylov subspace methods employ simple operations such as matrix-vector multiplications, these methods are deemed effective for the reduced-order modeling of large-scale sparse systems. However, Krylov subspace methods has its own set of limitations since there is no global error bound and no assurance that stability will be preserved in the reduced order model. When comparing balanced truncation to Krylov subspace methods, it is evident that using balanced truncation is a wiser choice when stability and error bound are a concern. Unlike Krylov subspace based methods, balanced truncation allows stability to be retained in the reduced-order model. However, Krylov subspace methods are more suitable than balanced truncation when numerical effort and storage requirements are in question.

3.2.1 | IRKA

Now that a general idea of Krylov subspace methods has been established, we can shift our attention to a specific Krylov based model reduction technique called Iterative Rational Krylov Algorithm, known as IRKA. This two-sided projection method is similar to the method presented in [38]. The work of this projection method is twofold. On one side, a Lyapunov equation is solved for the observability Gramian and on the other side, a moment-matching Krylov technique is applied. Consider a matrix $W \in C^{n\times n}$, a vector $u \in C^n$ and a point $\alpha \in C$, the Krylov space of index $j = 0, 1, 2, ...$ can be written as,

$$K_j(M, u, \alpha) := \mathrm{Im}([(\alpha I - M)^{-1}u, (\alpha I - M)^{-2}u, \ldots (\alpha I - M)^{-j}u]); \quad \text{if, } \alpha \neq \infty \tag{35}$$

The following theorem demonstrates how the moment matching problem can be solved with the help of Krylov projections.

Theorem 1. *If* $Im(V) = span[k_{j1}(A, B; \sigma_1) \ldots k_{jk}(A, B; \sigma_k)]$, *and*

$\mathrm{Im}(W) = \mathrm{span}\ [k_{jk+1}(A, B; \sigma_{k+1}) \ldots k_{j2k}(A, B; \sigma_{2k})]$, then j_k number of moments match between the transfer functions of the original and reduced order model at the interpolation point σ_k for $k = 1, ..., 2K$. For more information, we refer to [39] and the references therein.

4 | NUMERICAL ALGORITHMS

In this section, we delineate the necessary steps of the two model reduction techniques proposed in this paper. We see the implementation of balanced truncation and Krylov based IRKA in Algorithms 1 and 2 respectively.

4.1 | Algorithm 1: Balanced Truncation

The LRCF-ADI algorithm is comprised of the following steps. We use steps 1 to 4 to determine whether the Gramian we are working with is a controllability Gramian or an observability Gramian. Once decided, we move on to the next set of three steps to compute the low-rank Cholesky factors using the LRCF-ADI method. We can see that steps 6 to 8 are embedded in a loop where each time the loop is executed, a new column is added to the Cholesky factor. We continue this iteration process as soon as the approximate Cholesky factor Z_i in step 8 satisfies the relation in (19). Note that, in (19) $X_i \approx Z_i Z_i^T$ and Z_i is computed in step 8 after *i*-th iteration steps.

Algorithm 1.
Input: $\mathcal{A}$, $\mathcal{E}$, $\mathcal{B}$, $\mathcal{C}$ and shift parameters $\{p_1, p_2, ..., p_j\}$
Output: Z_i such that $Z_i = \breve{Z}_C$ in (20), or, $Z_i = \breve{Z}_o$ in (21). Also, $\breve{A}$, $\breve{E}$, $\breve{B}$, $\breve{C}$ and $\breve{\mathcal{H}}(s)$ for the ROM (28).

1. **IF** type (20)
2. $\mathcal{G} = \mathcal{B}$
3. **ELSE IF** type (21)
4. $\mathcal{G} = \mathcal{C}^T$ and $\mathcal{A} = \mathcal{A}^T$, $\mathcal{E} = \mathcal{E}^T$
5. **END IF**
6. $Z_1 = \sqrt{-2Re(p_i)}(\mathcal{A} + p_i\mathcal{E})^{-1}\mathcal{G}$
7. **FOR** $i = 2, ..., j$ **DO**
8. $Z_i = [Z_{i-1} \quad \sqrt{\frac{Re(p_i)}{Re(p_{i-1})}}(Z_{i-1} - (p_i + \overline{p_{i-1}})(\mathcal{A} + p_i\mathcal{E})^{-1}(\mathcal{A} - p_i\mathcal{E})Z_{i-1}]$
9. **END FOR**
10. **IF** type (20), $\breve{Z}_C = Z_i$
11. **ELSE IF** type (21), $\breve{Z}_O = Z_i$
12. $U_e\Sigma_e V_e^T = \mathrm{SVD}(\breve{Z}_O^T\mathcal{E}\breve{Z}_C)$
13. $T_L = \breve{Z}_O U_e \Sigma_e^{-1/2}$ and $T_R = \breve{Z}_C V_e \Sigma_e^{-1/2}$
14. $\breve{E} = T_L^T\mathcal{E}T_R, \quad \breve{A} = T_L^T\mathcal{A}T_R, \quad \breve{B} = T_L^T\mathcal{B}, \quad \breve{C} = \mathcal{C}T_R$
15. $\breve{\mathcal{H}}(s) = \breve{C}(s\breve{E} - \breve{A})^{-1}\breve{B}$
16. $||\mathcal{H}(s) - \breve{\mathcal{H}}(s)||_\infty$

In step 12, we find the economic singular value decomposition of the product matrix $\mathcal{E}$ with the two Cholesky factors. As a result, we obtain a diagonal matrix, the entries of which represent Hankel singular values. The two projection matrices T_L and T_R are constructed in step 13.

Applying these projection matrices to the system matrices, we can find the reduced order model as shown in step 14. The transfer function of the reduced order model is shown in step 15. Finally, we check the H_∞ norm bound in step 16 to verify the accuracy of the truncation. If the error is smaller than twice the sum of the truncated Hankel singular values, the truncation has been successfully accomplished.

4.2 | Algorithm 2: IRKA

The Krylov Based IRKA algorithm is initiated once the initial shifts are randomly selected. Using these shifts, we can create the right projection matrix $V \in \mathbb{R}^{\mathfrak{n}\times r_{kry}}$, as shown in step 2. Step 3 reflects the SVD portion of this two-sided projection method where the Lyapunov equation is solved to obtain an approximation of the observability Gramian Q. Moving on to step 4, we can see that the observability Gramian is required to compute the left projection matrix $W \in \mathbb{R}^{\mathfrak{n}\times r_{kry}}$. In step 5, the two projection matrices V and W are then used to construct $E_{r_{kry}}$ and $A_{r_{kry}}$.

Algorithm 2.
Input: $\mathcal{A}$, $\mathcal{E}$, $\mathcal{B}$, $\mathcal{C}$ and shift parameters $\{\delta_1, \delta_2, ..., \delta_i\}$
Output: $A_{r_{kry}}$, $E_{r_{kry}}$,$B_{r_{kry}}$,$C_{r_{kry}}$ and $H_{r_{kry}}$

1. **Select** initial shift δ_i for $i = 1, ..., r_{kry}$
2. $V = \mathrm{Im}[(\delta_1\mathcal{E} - \mathcal{A})^{-1}\mathcal{B}, ..., (\delta_{r_{kry}}\mathcal{E} - \mathcal{A})^{-1}\mathcal{B}]$
3. Solve $\mathcal{A}^T Q\mathcal{E} + \mathcal{E}^T Q\mathcal{A} = -\mathcal{C}^T\mathcal{C}$ to get Q
4. Choose $W = QV(V^TQV)^{-1}$
5. Set $E_{r_{kry}} = W^T\mathcal{E}V$ and $A_{r_{kry}} = W^T\mathcal{A}V$
6. Update V until convergence
   WHILE $\mathrm{real}(\lambda_i E_{r_{kry}} - A_{r_{kry}}) < 0$ **DO**
   i) $\delta_i \leftarrow (\lambda_i E_{r_{kry}} - A_{r_{kry}})$
   ii) Compute step (2)
   END WHILE
7. Update W using step 4
8. Update $E_{r_{kry}} = W^T\mathcal{E}V$, $A_{r_{kry}} = W^T\mathcal{A}V$, $B_{r_{kry}} = W^T\mathcal{B}$, $C_{r_{kry}} = \mathcal{C}V$
9. Produce $H_{r_{kry}} = C_{r_{kry}}(sE_{r_{kry}} - A_{r_{kry}})^{-1}B_{r_{kry}}$

The performance and rate of convergence of this algorithm is governed by the shifts δ_i. For better performance, the shifts δ_i are updated using step 6. The condition real $(\lambda_i E_{r_{kry}} - A_{r_{kry}}) < 0$ is used to locate the eigenvalues of the pencil that possess negative real part. These negative real eigenvalues are then substituted as δ_i and step 6 is repeated until a satisfactory reduced order model is obtained in terms of the reduced transfer function. In step 7, W is modified according to the new projection matrix V. It is worth mentioning that since the negative real eigenvalues of the pencil were used to create the projection matrices V and W, we are able to ensure the stability of the reduced model. In step 8, the reduced order matrices $E_{r_{kry}}$, $A_{r_{kry}}$, $B_{r_{kry}}$ and $C_{r_{kry}}$ are computed. The final step of the algorithm consists of generating the transfer function of the reduced-order model.

5 | NUMERICAL RESULTS

The accuracy and performance of our two proposed algorithms are tested using data that is produced from a RF circuit simulator. This circuit simulator is composed of 5 nodes. To discretize the time-varying system, a total of 129 time steps are used. To perform the steady state analysis of the system, a period of $T = 4ms$ is considered. The discretized system has a dimension of 645×645.

For our balanced truncation-based algorithm, we start off by using the block Arnoldi method to locate the large eigenvalues of the system. Likewise, the inverse block Arnoldi method is utilized to locate the small eigenvalues. Two variables B_a and B_i are assigned to denote the number of iterations for the block Arnoldi method and inverse Arnoldi method, respectively. For convenience, we assign $B_a = 25$ and $B_i = 20$ while keeping in mind that the order of the system must be significantly larger than the number of iterations ($k << \mathfrak{n}$). In addition, we also have to make sure that the sum of B_a and B_i is larger than $2S_o$, where S_o denotes the number of shift parameters for the LRCF-ADI method. Setting $S_o = 20$ and the residual tolerance level ϵ in (19) to 10^{-5} results in the convergence of the LRCF-ADI method. The iterative process continues to run until this residual tolerance level is met. The original LTI system has an order of $\mathfrak{n} = 645$. For convenience, we assumed $\mathcal{C} = \mathcal{B}^T$. Applying balanced truncation to the original LTI system gives us a reduced model of order 10.

For the Krylov based IRKA algorithm, we begin the algorithm using 10 arbitrary δ_i values. Using these randomly chosen δ_i shifts, the right projection matrix V is built and subsequently, the left projection matrix W is created as well. Once the negative real eigenvalues of the system are computed, these eigenvalues are assigned as the new δ_i shifts. The projection matrices V and W are updated according to the new δ_i shifts. Setting the residual tolerance level for the IRKA algorithm to 10^{-5} and running the algorithm for a total of 10 iterations results in the convergence of the algorithm as desired. Applying the Krylov based IRKA algorithm to the main model gives us a reduced model of order 13.

Figure 1 illustrates the structural sparsity of the system matrices $\mathcal{E}$ and $\mathcal{A}$. Since $\mathcal{E}$ is a singular matrix, we are unable to find the inverse in the conventional way. Instead, we adopt the concept of pseudo-inverse to determine the inverse. Due to the complex nature of the Ritz values found from the block Arnoldi and inverse Arnoldi

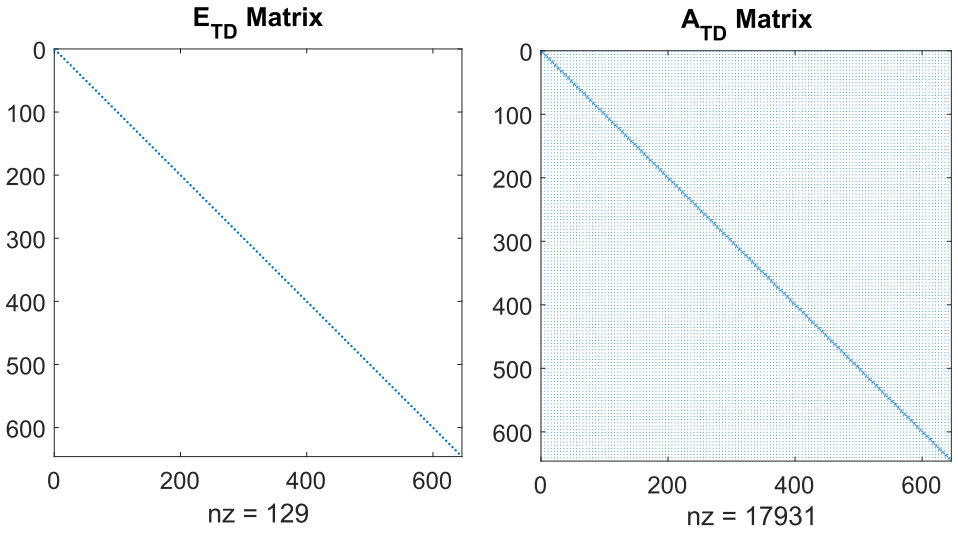

FIGURE 1 $\mathcal{E}$ and $\mathcal{A}$ Matrices of the system [Color figure can be viewed at wileyonlinelibrary.com]

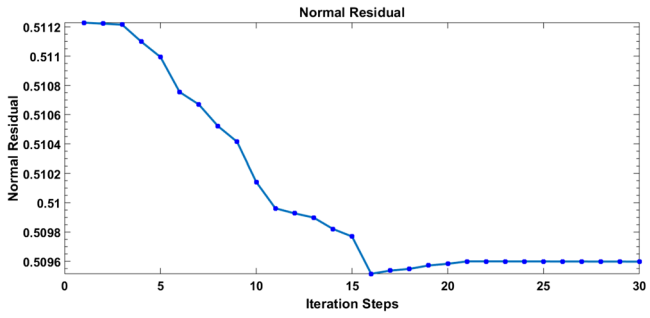

FIGURE 2 Normal residual of LRCF-ADI [Color figure can be viewed at wileyonlinelibrary.com]

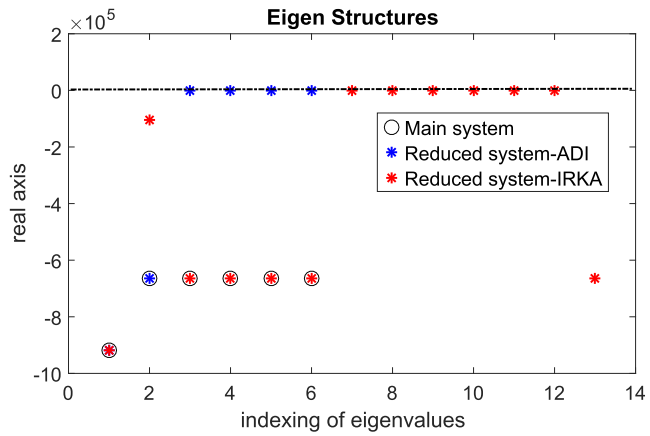

FIGURE 3 Eigen structures of the main and reduced systems [Color figure can be viewed at wileyonlinelibrary.com]

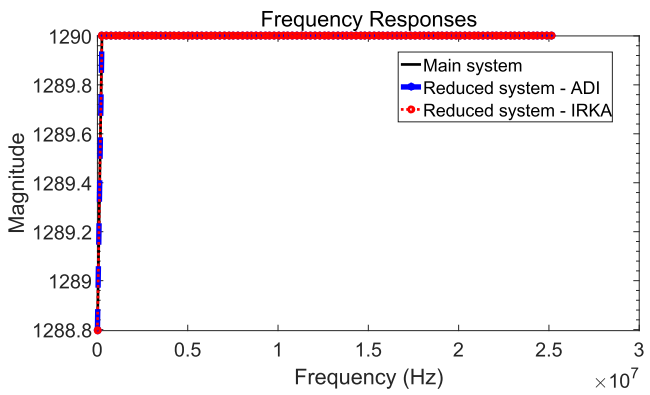

FIGURE 4 Frequency responses of original and reduced systems [Color figure can be viewed at wileyonlinelibrary.com]

method, the shift parameters for the LRCF-ADI method are not optimal.

The residual obtained in each iteration of the LRCF-ADI method is shown in Figure 2.

In Figure 3 we depicted the real part of few eigenvalues (of largest magnitudes) for the main system and for the two reduced systems. According to Figure 3, we can see that the eigenvalues of the main system and the two reduced systems are located on the open left half plane. As mentioned earlier, this particular scenario verifies the stability of a system. Therefore, we can state that the main system and its two corresponding reduced models are stable. We observe that a good number of the eigenvalues of the ADI-induced system and the IRKA-induced system completely overlap with the main system's eigenvalues. We notice that few eigenvalues of both the reduced system are located at very close to the zero border line (dot-solid line in Figure 3).

One of the most important criteria for comparing the accuracy of a reduced-order model is to find its frequency response. The dynamics of a system can be described by showing its frequency response. The transfer functions of the main system, the balanced truncation based reduced system, and the IRKA based reduced system are represented as $\mathcal{H}(s) = \mathcal{C}(s\mathcal{E} - \mathcal{A})^{-1}\mathcal{B}$, $\breve{\mathcal{H}}(s) = \breve{\mathcal{C}}(s\breve{\mathcal{E}} - \breve{\mathcal{A}})^{-1}\breve{\mathcal{B}}$ and $H_{r_{kry}} = C_{r_{kry}}(sE_{r_{kry}} - A_{r_{kry}})^{-1}B_{r_{kry}}$ respectively. Here, s denotes the complex frequency. Figure 4 displays the

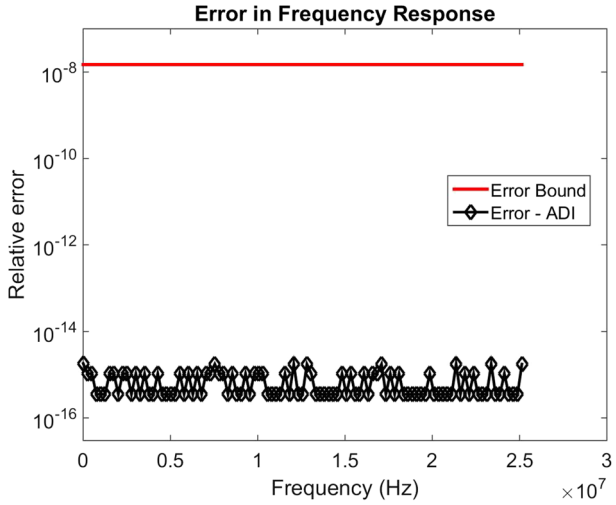

FIGURE 5 Error and error bound in frequency response for balanced truncation MOR [Color figure can be viewed at wileyonlinelibrary.com]

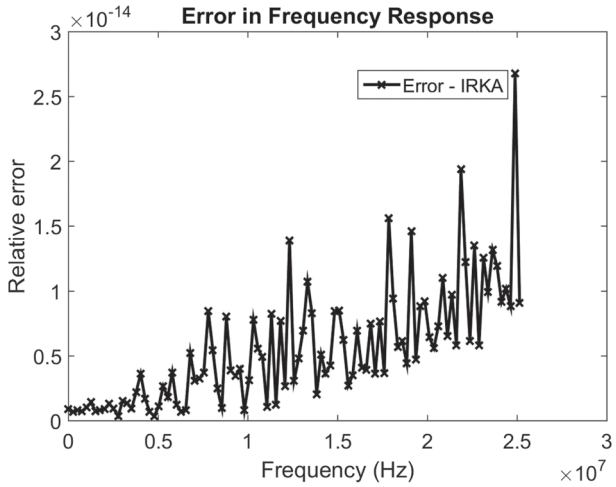

FIGURE 6 Error in frequency response

frequency responses of all three systems over the frequency range $4 \times 10^{-6} - 4 \times 10^{6}$.

Figure 5 illustrates the error in the frequency responses of the original (main) system and the reduced-order system obtained via the balanced truncation approach. The frequency varies from 0 Hz to 30 MHz. The graph reveals that the error is bounded by the the relation (29), which is one of the crucial demands in the balancing based reduction method.

Figure 6 illustrates the similar error plot for the frequency responses of the original (main) system and Krylov based MOR. Here we can not guarantee the error bound since IRKA does not provide any error bound relation for the reduced model. But the graph reveals that the error is of satisfactory level.

The accuracy of our model reduction techniques is illustrated by plotting the Bode plots for the main system and

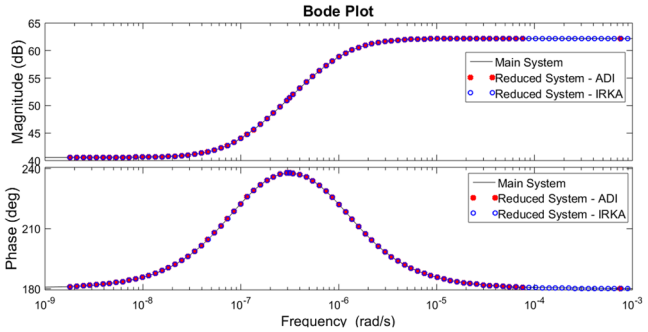

FIGURE 7 Bode plots of the main and reduced systems [Color figure can be viewed at wileyonlinelibrary.com]

for the two reduced systems. The Bode plots of the original, ADI-reduced, and IRKA-reduced systems are shown in Figure 7. Bode plots are a great way to display the gain and phase response of a system for various frequencies. Based on Figure 7, it is evident that the magnitude response of the main system and the two reduced systems overlap. Similar results are observed in the phase plot of the three systems.

6 | CONCLUSION

In recent years, model order reduction of linear and nonlinear systems has sparked great interest amongst engineers and mathematicians and has become a popular topic of active research. This interest was triggered by the growing need to accurately and efficiently represent complex and large-scale mathematical models. Model order reduction serves as an important tool to overcome the challenges associated with the numerical simulation and optimization of these complicated mathematical models. The aim of this paper was to develop two iterative methods that could be used to reduce the dimensions of a real-life large-scale LTV system. We started with a LTV system that was reformulated to a LTI system and the resulting LTI system had a dimension of 645×645. After applying our proposed balanced truncation technique, we obtained a reduced-order model of order 10. Similarly, we obtained a reduced-order model of order 13 after applying the Krylov based IRKA algorithm to the original LTI system. Based on our numerical results, we are able to conclude that the two reduced order models are stable at a certain frequency range: 0 Hz to 30 MHz. Furthermore, the errors generated from the two reduced models in the above frequency range remain within the satisfactory levels.

The paper has some limitations. This paper's focus is LTV models that are weakly nonlinear and permit a discretized stable LTI reconstruction. But there are many mathematical models generated from real life systems that are simply unstable. A common investigation for model

reduction of such systems in discrete-time setting is to decompose the unstable system into causal and noncausal parts and explore the treatment of model reduction techniques for both parts separately [40]. It remains a future research direction for us.

Another issue for further consideration is the shift parameters that were used in the LRCF-ADI iteration were suboptimal due to the complex nature of the Ritz values. Using optimal parameters in the LRCF-ADI method will yield better convergence results. Also, a better initial shift selection for the Krylov based IRKA algorithm can lead to a better approximation of the original model. Minimizing the residual is subject to further study.

ACKNOWLEDGEMENTS

Funding information North South University research grant: NSU-RP-18-040/2018-2019.

ORCID

Mohammad-Sahadet Hossain https://orcid.org/0000-0002-7953-1351
Aniqa Tahsin https://orcid.org/0000-0003-3440-5105

REFERENCES

1. Z. Bai, *Krylov subspace techniques for reduced-order modeling of large-scale dynamical systems*, Appl. Numer. Math. **43** (2002), no. 1-2, 9–44.
2. A. C. Antoulas, *An overview of approximation methods for large-scale dynamical systems*, Annu. Rev. Control. **29** (2005), no. 2, 181–190.
3. H. Hamdi, M. Rodrigues, C. Mechmeche, and N. Benhadj Braiek, *Fault diagnosis based on sliding mode observer for LPV descriptor systems*, Asian. J. Control. **21** (2019), no. 1, 89–98.
4. R. Telichevesky, K. Kundert, and J. White, *Efficient AC and noise analysis of two-tone RF circuits*, 33rd Design Automation Conference Proceedings, Las Vegas, NV, USA, 1996.
5. M. S. Hossain and P. Benner, *Projection-based model reduction for time-varying descriptor systems: New results*, Numer. Algebr. Control & Optimization **6** (2016), no. 1, 73–90.
6. J. Roychowdhury, *Reduced-order modeling of linear time-varying systems*, Ieee/acm international conference on computer-aided design, San Jose, CA, USA, 1998.
7. J. R. Phillips, *Projection-based approaches for model reduction of weakly nonlinear, time-varying systems*, IEEE T. Comput.-Aid D. **22** (2003), no. 2, 171–187.
8. A. Varga, *Balanced truncation model reduction of periodic systems*, 33rd Design Automation Conference Proceedings, Sydney, Australia, 2000.
9. K. S. Haider, A. Ghafoor, M. Imran, and F. M. Malik, *Model reduction of large scale descriptor systems using time limited gramians*, Asian. J. Control. **19** (2017), no. 3, 1217–1227.
10. V. Mehrmann and T. Stykel, *Balanced truncation model reduction for large-scale systems in descriptor form*, Lect. Notes. Comput. Sci. Eng. Dimens. Re. Large-Scale. Syst. **45** (2005), 83–115.
11. T. Stykel, *Gramian-based model reduction for descriptor systems*, Math. Control Signal. Syst. **16** (2004), no. 4, 297–319.
12. A. G. Muhammad Imran, *Model reduction of descriptor systems using frequency limited gramians*, J. Franklin Inst. **352** (2015), no. 1, 33–51.
13. E. J. Grimme. (1997). *Krylov projection methods for model reduction*, Ph.D. Thesis, University of Illinois, Urbana, Urbana, Illinois.
14. R. W. Freund, *Model reduction methods based on Krylov subspaces*, Acta Numer. **12** (2003), 267–319.
15. S. Gugercin, A. C. Antoulas, and C. A. Beattie, *H_2 model reduction for large-scale linear dynamical systems*, SIAM J. Matrix Anal. Appl. **30** (2008), 609–638.
16. B. Salimbahrami and B. Lohmann, *Krylov subspace methods in linear model order reduction: Introduction and invariance properties*, 2002. Sci. Rep. Inst. of Automation.
17. D. Kumar and V. Sreeram, *Factorization-based frequency-weighted optimal Hankel-norm model reduction*, Asian J. Control. (2019), 1–13. https://doi.org/10.1002/asjc.2096
18. Q. Su, V. Balakrishnan, and C. Koh, *Efficient approximate balanced truncation of general large-scale RLC systems via Krylov methods*, Proceedings of asp-dac/vlsi design, 7th Asia and South Pacific Design Automation Conference 15th International Conference on Vlsi Design Proceedings, 2002, pp. 311–316.
19. T. Wolf, H. Panzer, and B. Lohmann, *Model order reduction by approximate balanced truncation a unifying framework*, At-Autom. **61** (2013), no. 8, 545–556.
20. S. Gugercin, *An iterative SVD-Krylov based method for model reduction of large-scale dynamical systems*, Linear Alg. Appl. **428** (2008), no. 8-9, 1964–1986.
21. S. Gugercin and A. C. Antoulas, *Model reduction of large-scale systems by least squares*, Linear Algebra Appl. **415** (2006), no. 2-3, 290–321.
22. K. A. Gallivan, E. Grimme, and P. M. V. Dooren, Model reduction of large-scale systems rational Krylov versus balancing techniques, *Error Control and Adaptivity in Scientific Computing*, Springer, Dordrecht, 1999, pp. 177–190.
23. B. Besselink, U. Tabak, A. Lutowska, N. van de Wouw, H. Nijmeijer, D. J. Rixen, M. E. Hochstenbach, and W. H. A. Schilders, *A comparison of model reduction techniques from structural dynamics, numerical mathematics and systems and control*, J. Sound Vibr. **332** (2013), no. 19, 4403–4422.
24. S. Liu, P. W. Sauer, D. Chaniotis, and A. Pai, *Krylov subspace and balanced truncation methods for power system model reduction*, Vol. **94**, Springer, New York, 2013, pp. 119–142.
25. W. Witteveen, Comparison of CMS, Krylov and balanced truncation based model reduction from a mechanical application engineer's perspective, *Topics in Experimental Dynamics Substructuring and Wind Turbine Dynamics*, R. Mayes, (ed.), Springer, New York, 2012, pp. 319–331.
26. L. A. Zadeh, *Frequency analysis of variable networks*, IEEE Transactions on Circuits and Systems, 1950.
27. R. Eid. (2009). *Time domain model reduction by moment matching*, Master's Thesis, Technische Universität Munchen.
28. S. Savov, *Solution bounds for algebraic equations in control theory*, Prof. Marin Drinov Academic Publishing House, Sofia, 2014.
29. M. Hajarian, *Matrix form of biconjugate residual algorithm to solve the discrete-time periodic sylvester matrix equations*, Asian J Control **20** (2018), no. 1, 49–56.

30. J.-R. Li and J. White, *Low rank solution of Lyapunov equations*, SIAM J. Matrix. Anal. Appl. **24** (2002), 260–280.
31. M. S. Hossain. (2011). *Numerical methods for model reduction of time-varying descriptor systems*, Ph.D. Thesis, University of Technology, Germany.
32. T. Penzl, *A cyclic low rank smith method for large sparse Lyapunov equations with applicatins in model reduction and optimal control*, SIAM J. Sci. Comput. **21** (1999), 1401–1418.
33. P. Benner, M. S. Hossain, and T. Stykel, Model reduction of periodic descriptor systems using balanced truncation, *Model reduction in circuit simulation*, P. Benner, M. Hinze, and J. ter Maten, (eds.), Lecture Notes in Electrical Engineering, Vol. **74**, Springer-Verlag, Berlin, Heidelberg, 2011, pp. 187–200.
34. M. H. Likhon, S. Arifeen, and M. S. Hossain, *Model order reduction of continuous LTI large descriptor system using LRCF-ADI and square root balanced truncation*, World Congress on Engineering, Vol. **1**, London, UK, 2015.
35. G. Golub and W. Kahan, *Calculating the singular values and pseudo-inverse of a matrix*, SIAM J. Numer. Anal. **2** (1965), 205–224.
36. L. N. Trefethen and D Bau, *Numerical linear algebra*, Society of Industrial and Applied Mathematics, Philadelphia, USA, 1997.
37. S. Gugercin and A. C. Antoulas, *A survey of model reduction by balanced truncation and some new results*, Int. J. Control **77** (2004), no. 8, 748–766.
38. S. Gugercin, *An iterative SVD-Krylov based method for model reduction of large-scale dynamical systems*, IEEE Conference on Decision and Control, and the European Control Conference, Seville, Spain, 2005.
39. A. Rahman and M. S. Hossain, *SVD-krylov based model reduction for time-varying periodic descriptor systems*, 2nd international conf. on electrical engineering and information & communication technology (iceeict), Dhaka, Bangladesh, 2015.
40. P. Benner and M. S. Hossain, *Structure preserving iterative methods for periodic projected lyapunov equations and their application in model reduction of periodic descriptor systems*, Numer. Algorithms **76** (2017), no. 4, 881–904.

AUTHOR BIOGRAPHIES

Mohammad Sahadet Hossain received his Ph.D. from Chemnitz University of Technology, Germany, in 2011. He then undertook postdoctoral research at the Max-Planck Institute for Dynamics of Complex Technical Systems, Magdeburg, Germany, from 2011 to 2012. Since August 2012, he has been working as a full time faculty member at the School of Electrical and Computer Engineering, North South University, Dhaka, Bangladesh. North South University, Dhaka, Bangladesh. Currently he is working as an associate professor at the Department of Mathematics and Physics of that university. His research interest includes linear periodic and standard control systems, model reduction, iterative solvers for periodic matrix equations, and high performance computing.

Aniqa Tahsin is currently a graduate student studying telecommunications at the Volgenau School of Engineering, George Mason University, Virginia, USA. She completed her undergraduate degree in electrical and electronic engineering from North South University, Dhaka, Bangladesh in 2018. Aniqa's research interests are model order reduction and wireless communications with an emphasis on 5G.

Sufi Galib Omar completed his Bachelor degree in electrical and electronic engineering with a major in solid state electronics from North South University, Dhaka, Bangladesh in 2017. He since worked as a part-time lab officer at the same department from 2018–2019. His research interest includes control systems, control engineering, communication, robotics, network securities, and artificial intelligence.

Ekram H. Khan is currently pursuing his M.S. degree in micro- and nanotechnologies at Ilmenau University of Technology, Germany. He received his B.S. degree in electrical and electronic engineering from the North South University, Dhaka, Bangladesh, in 2017. His research interests include linear control systems, model reduction, and nanoelectronics.

How to cite this article: Hossain M-S, Tahsin A, Omar SG, Hossain Khan E. Comparative analysis of model reduction strategies for circuit based periodic control problems *Asian J Control*. 2021;23: 1512–1523. https://doi.org/10.1002/asjc.2312